J. Membrane Biol. 102, 1–10 (1988)

The Journal of
Membrane Biology

Surface Charge Near the Cardiac Inward-Rectifier Channel Measured from Single-Channel Conductance

Michael J. Kell and Louis J. DeFelice
Department of Anatomy and Cell Biology, Emory University School of Medicine, Atlanta, Georgia 30322

Summary. The conductance of a channel to permeable ions depends on the number of ions near the mouth of the pore. Surface charge controls the local concentration, and impermeable cations can modify this charge. Correlating channel conductance with the concentration of impermeable cations therefore determines the local charge near the open pore. This paper presents data from cell-attached patches on embryonic chick ventricle cells, and it uses the conductance of inward-rectifier channels in the patch (in 100 mM K, with various concentrations of Na, Ca, Ba, and Mg) to estimate the local surface potential. The results indicate the presence of ionized residues near the mouth of the channel. Using the Boltzmann equation and the Gouy-Chapman relation, the surface potential due to these residues (in 100K/33Na/0Ca/0Ba/0Mg) is −40 mV, and the charge density is −0.25 e/nm^2.

Key Words potassium channels · inward-rectifier · heart cells · surface charge

Introduction

Sakmann and Trube (1984*a*,*b*), using the patch-clamp technique (Hamill et al., 1981), first identified inward-rectifier channels in adult ventricle cells from the guinea pig heart. The channel showed many similarities to the macroscopic inward-rectifier (or anomalous-rectifier) current in mammalian ventricle, including a high selectivity for K ions. The current, also designated by I_{K1} or I_{bg}, exists in many different kinds of cells; Beeler and Reuter (1977) and McDonald and Trautwein (1978*a*,*b*) were among the first to describe this current in cardiac tissue. The role usually ascribed to I_{K1} is that it helps determine the resting conductance and assists in the repolarization of the cardiac action potential.

Sakmann and Trube estimated that in guinea pig ventricle the inward-rectifier had a density of 1 channel/2 μm^2, and in high external K the pore exhibited interconverting substates with distinct conductances. Numerous single-channel studies now exist; in adult cardiac tissue, these include Bechem, Glitsch and Pott (1983, guinea pig atrium), Kameyama, Kiyosue and Soejima (1983, rabbit ventricle), Trube and Hescheler (1984, guinea pig ventricle), Kurachi (1985, guinea pig ventricle), and Hume and Uehara (1985, guinea pig atrium and ventricle). The embryonic chick heart ventricle inward (anomalous)-rectifier (designated AR) shares many properties with previously described channels in adult tissue: it is K-selective, conducts primarily when the potential is negative to E_K, and has at least five conduction states in high external K.

The present work is an attempt to study the density of charge near an open channel using the conductance of the AR channel as an assay. Varying the concentration of impermeable cations, while holding the concentration of the permeable K ions constant, changes the conductance of the AR pore. We interpret this effect as a change in the local K available to the channel. Under this assumption, the surface potential is calculable from the Boltzmann equation and the surface charge from the Gouy-Chapman relation. One difficulty arises, for if local K varies as the calculations suppose, not only conductance but also driving force will change. The new driving force has a separate influence on the current, making the calculations more complex. To avoid this problem, McLaughlin, Szabo and Eisenman (1971) changed the impermeable ions equally on both sides of the membrane, leaving the driving force constant. Instead, we measured open channel $i(V)$ curves, in which the conductance of the pore and its reversal potential are easily separated for any condition.

Using channel conductance to measure surface charge has advantages over other methods: (i) it requires essentially no assumptions about channel kinetics; (ii) it is relatively free of the uncertainty, present in virtually all macroscopic experiments, that the measured current comes about from a single class of channel; (iii) only the patch encounters the test solutions; (iv) surface charge emerges from a single parameter (*cf.* Apell et al., 1979*a*,*b*),

whereas macroscopic experiments relate the charge to multi-parameter effects, such as voltage shifts of peak current (Frankenhaeuser & Hodgkin, 1957; Gilbert & Ehrenstein, 1969; Hille, Woodhull & Shapiro, 1975; Schauf, 1975).

Materials and Methods

Preparation of ventricular cells by enzymatic digestion of 7-day chick hearts followed the procedure of DeHaan (1967). Clusters of two to eight spontaneously beating cells adhere to Falcon 1008 styrene petri dishes. The cells were usually cultured for at least one day before exchanging the medium for a protein-free, salt solution and moving the cells to the patch-clamp setup. The bath solution, 3.5 K/130 choline, contained (in mM) 130 choline, 3.5 K, 1.5 Ca, 0.5 Mg, 133.5 Cl, 2 SO_4, 1 H_2PO_4, 5 dextrose, and 10 HEPES (pH 7.35) and was isosmotic to the cell at 270 mOsm: this solution arrested beating within minutes and gave the cell a constant resting potential, measured independently under current clamp. About half the cells are naturally quiescent.

Patch pipettes were made from borosilicate glass. Storing the glass at 470°C for 24 hr before using it increases its surface energy by removing entrapped gases and surface organics. This treatment provided a simple and clean storage facility, and it improved the glass for use as patch electrodes. Electrode resistances were between 3.4 and 6.9 MΩ (95% confidence limits, n = 31). Assuming that the patch electrode isolated a hemispherical segment of the membrane (Sakmann & Neher, 1983), the area of the patch is between 5 and 6 μm^2.

The solution in the patch electrode was under slight positive pressure (less than 4 cm H_2O) as the electrode moved toward the cell surface and formed the mechanical seal. Upon applying a slight suction (−4 cm H_2O), a resistance of 10-100 GΩ developed within seconds. This procedure maintained the composition of the electrode solution during the sealing process.

All pipette solutions contained 10 mM HEPES (acid) at pH 7.4. The divalent-free solutions also included 5 mM EGTA (acid), which was sufficient to buffer the Ca that might be contaminating the pipette solution during the formation of the patch or the Ca that is bound to the external surface of the membrane (*see* Schmid & Reilley, 1957). Divalent-free solutions without EGTA gave similar results in a few trials. All experiments (except Fig. 3) used 100 mM K in the patch pipette.

Monitoring the cell resting potential with electrodes containing an intracellular-like solution gave an average resting potential (in 3.5 K/130 Na) of −69.0 ± 4.4 mV (1 SD, n = 21). With choline replacing Na, cells depolarized to −48.4 ± 5.3 mV (1 SD, n = 21). This change was reversible. Resting potentials were constant for hours in either 3.5 K/130 Na or 3.5 K/130 choline. Reversible K channel blocking could account for the depolarization in choline; whatever the solution, we used the resting potential to calculate the absolute voltage across the patch. Bath temperature was 23–25°C. A List EPC5 amplifier in voltage clamp or current clamp monitored the current or the voltage, which we collected and stored on floppy disks on a Nicolet 4094 oscilloscope and analyzed later on an HP 9826 computer.

Analysis

Substates

Most patches contained several current levels for the same pipette conditions. Multiple levels occur if there are different kinds of channels in the patch; they could also result from a channel with substates. In analyzing records like Fig. 4, we start with the smallest current and find its multiples. We then locate the next level (not an addition of the first) and its multiples, continuing until all steps in a given record classify as unique conduction states or as additions of these states. Ignoring the latter, the tiers could represent either dissimilar channels or substates of similar channels; we refer to the levels as substates because transitions between them often occurred within 100 μsec (the limit set by the 1.6 kHz cutoff). However, we made no statistical test for the independence of the steps and cannot say whether the unmatched plateaus in a given record represent substates of connected channels or unique states of autonomous channels. We identified five disparate levels by the above procedure, plotted them separately, and established their dependence on the concentration of the impermeable ions in the pipette.

Surface Potentials

Boltzmann's equation gives the surface concentration of the permeable ion (C_0) in terms of its bulk concentration (C_b) and the surface potential of the membrane (ϕ_0):

$$C_0 = C_b \exp(-ze\phi_0/kT) \tag{1}$$

where kT is the thermal energy, and ze is the charge of the permeable ion. If the single-channel conductance (γ) is proportional to the first power of the surface concentration of K, then it follows from Eq. (1) that

$$\gamma/\gamma_n = \exp[-ze(\phi_0 - \phi_n)/kT] \tag{2}$$

where γ_n is the value of γ in an uncharged membrane, and ϕ_n is the value of ϕ_0 in an uncharged membrane (zero). We approximated the condition of membrane neutrality by using concentrations of divalent cations high enough to saturate their lessening of channel conductance (*see* Apell et al., 1977, 1979*a*,*b*). Taking the logarithm of both sides of Eq. (2), setting ϕ_n + 0, and solving for ϕ_0 gives

$$\phi_0 = -(kT/ze)\ln(\gamma/\gamma_n). \tag{3}$$

If γ is proportional to a power of K other than one, the power divides the expression for ϕ_0.

Surface Charge

The Gouy-Chapman theory of the diffuse electric double layer gives an estimate of the surface charge, σ_s, from the surface potential, ϕ_0 (Grahame, 1947). With σ_s in e/nm² and ϕ_0 in mV, the relationship is

$$\sigma_s = 0.321\ \Sigma m_i[\exp(-z_i e\phi_0/kT) - 1]^{1/2}. \tag{4}$$

In Eq. (4), e is electronic charge, m_i is in units of moles/liter, z_i is the valence of the ith ion, and e/kT = 25.7 mV at 25°C.

Results

Single-Channel Conductance

Figure 1 shows the simplest condition, a single conductance level subject to symmetrical hyperpolar-

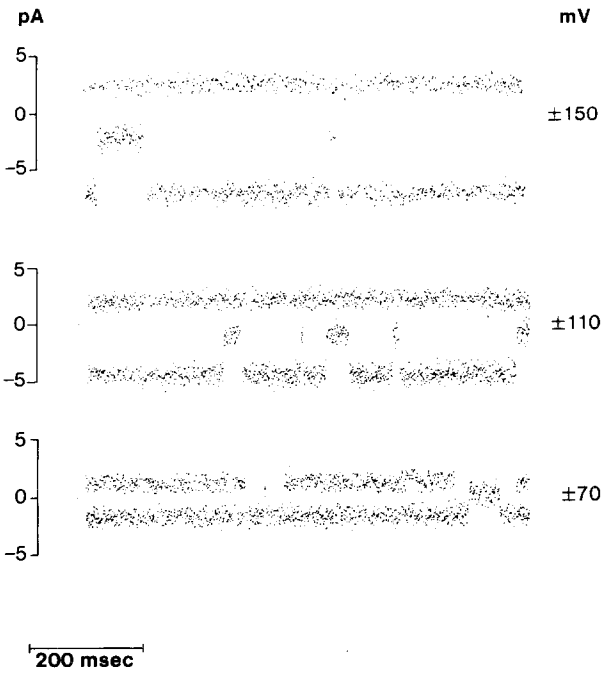

Fig. 1. Raw data for substate AR_5. Bath solution (in mM): 3.5 K, 130 choline, 10 HEPES (pH 7.35). Pipette solution: 100 K; 33 Na; 0 Ca; 10 Mg; 10 HEPES (pH 7.4). The values in the right-hand column signify the voltage across the channel, $V_{rest} - V_{pipette}$. A downward deflection is a channel opening. For positive values of voltage, the channel is closed (upper trace, each panel). We inserted gaps in the +70 mV trace in order to show channel closings in the −70 mV trace. The cutoff frequency is 1.6 kHz

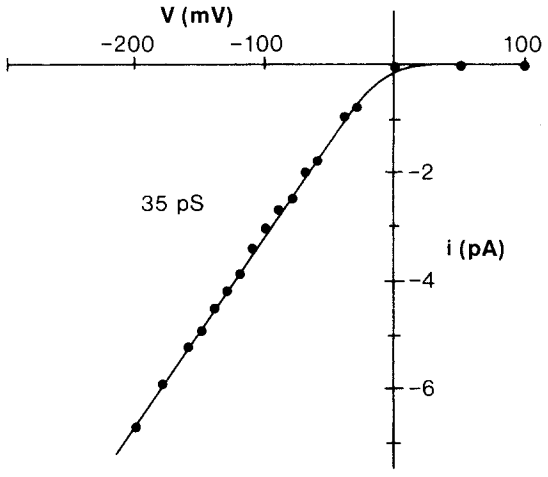

Fig. 2. The $i(V)$ curve for AR_5, from the data in Fig. 1. The current levels represent average values through the noisy traces

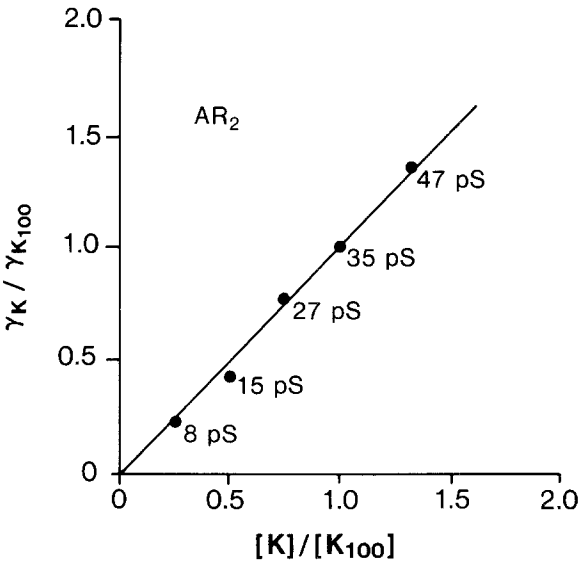

Fig. 3. The relation between conductance and pipette K for AR_2. The abscissa is the ratio of the conductance at a particular K concentration to the conductance at 100 mM K; the ordinate is the ratio of that particular K concentration to 100 mM K. Ionic strength remains constant by substituting Na for K. The line through the points has a slope of one for this substate. The pipette contains X mM K, (133-X) mM Na, 5 mM EGTA, and 10 mM HEPES (pH 7.4)

izations (−) and depolarizations (+) from rest. The conductance (in this case, AR_5) strongly rectifies, passing current only when the transmembrane potential is negative to the K reversal potential. Reversal lies close to zero mV because the pipette contains 100 mM K, about equal to the free K in 7 + 1 day embryonic ventricular cells [83 mM by ion-selective electrodes (Fozzard & Sheu, 1980) and 138 mM by flame photometry (McDonald & DeHaan, 1973).

Figure 2 gives the $i(V)$ curve for Fig. 1: V is the difference between the resting potential and the pipette potential. The conductance (γ_K = 35 pS, substate AR_5) remains constant between −200 and −20 mV and rectifies strongly above −20 mV. There is no outward current up to +200 mV. All substates have similar curves, in which the inward conductance depends on the concentration of K ions and the concentration of impermeable monovalent and divalent cations in the pipette.

Selectivity

The evidence that all AR conductance states are highly selective for K over Na, choline, divalent cations, and Cl is as follows: (i) no AR-like channels appear in the patches unless the patch pipette contains K; (ii) the inward conductance of all AR substates decreases as external K decreases (the smallest detectable substate, AR_5, is 4 pS in 3.5 K/130 Na/0 Ca/0 Mg/10 HEPES, pH 7.4); (iii) replacing Na by choline (leaving K = 100 mM) does not change any of the substate conductances; (iv) AR conductance of AR_2 is directly proportional to the concentration of K in the pipette (maintaining total ionic strength at 133 mM by substituting Na for K). Figure 3 shows this proportionality by plotting the

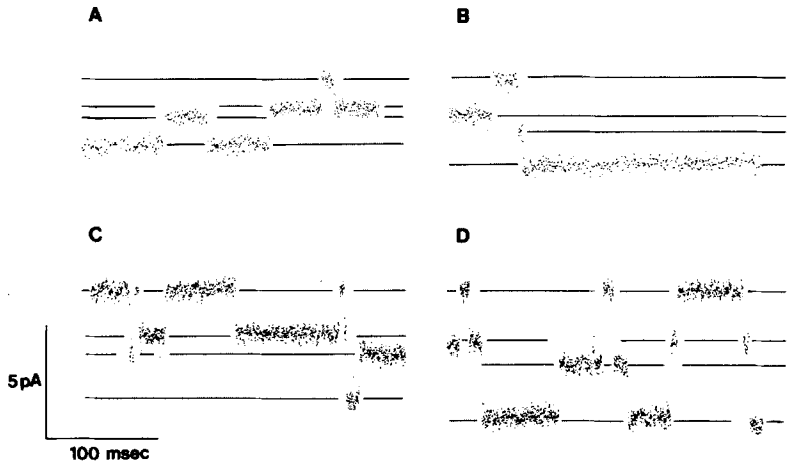

Fig. 4. Raw data from a patch containing more than one substate. There are four hyperpolarizations to −90 (*A*), −110 (*B*), −130 (*C*), and −150 (*D*) in mV. Bath solution (in mM): 3.5 K, 130 choline, 10 HEPES (pH 7.35). Pipette solution (in mM): 100 K, 33 Na, 0 Ca, 1 Mg, 10 HEPES (pH 7.4)

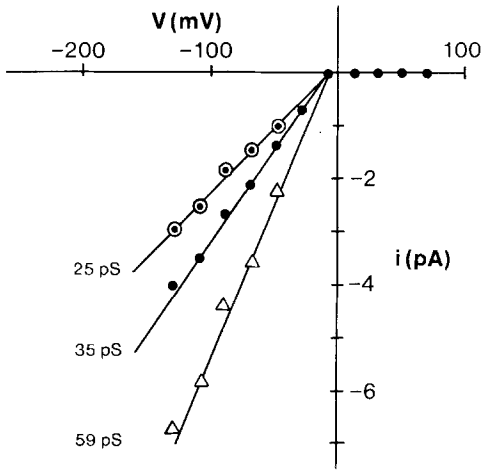

Fig. 5. The $i(V)$ curves for the patch in Fig. 4 containing two substates, AR_2, (25 pS) and AR_3 (35 pS), and the sum of these two substates (59 pS)

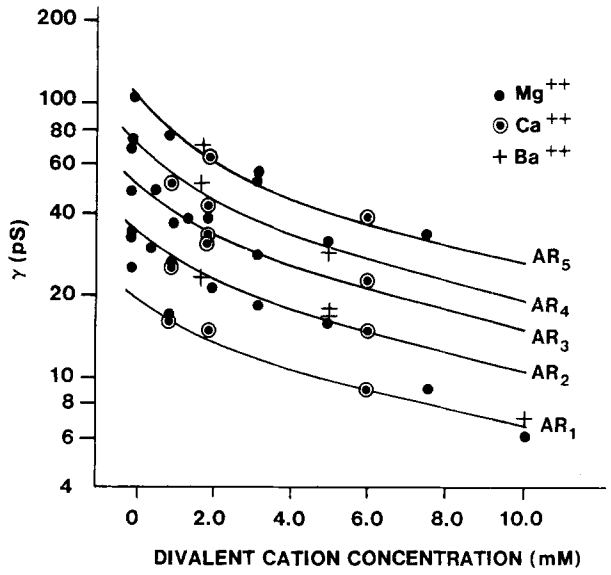

Fig. 6. Effect of divalent cation concentration on substate conductance. The points represent individual measurements, not mean values. The lines are empirical fits by eye. Most patches contain at least two substates. All pipette solutions contain 100 mM K and 33 mM Na

normalized conductance (γ_K/γ_{K100}) *vs.* normalized concentration (K/K_{100}) where K_{100} = 100 mM external potassium.

Substates

Figures 4 and 5 present a patch containing three different conductance levels. In this example, no instantaneous openings or closings occurred that would identify the highest and lowest conductances as conversions. An interpretation of Fig. 4 is that there are two separate channels in the patch, each expressing a different substate (AR_2 = 25 pS, AR_3 = 35 pS), and that these substates add to give the top level. (We adopt the term substate for convenience only; *see* the section on substates in Analysis.) Figure 5 plots the $i(V)$ curves for the two substates and for the addition state. The common intercept of the extrapolated curves indicates that the two conductances have the same selectivity.

Divalent Cations and Channel Conductance

Figure 6 summarizes the conductances of five substates from 33 patches as a function of the concentration of three impermeable divalent cations. The monovalent cation concentrations were 100 K and 33 Na in all experiments, resulting in solutions of nearly equivalent ionic strength. The lines in Fig. 6 sort the data into five groups. Conductance decreases monotonically with increasing bulk divalent cation concentration (McLaughlin et al., 1971; Apell et al., 1977, 1979*a*,*b*; Bell & Miller, 1984). For one of the substates, AR_1, data exist out to 40 mM

Table 1. Substate conductance ratios *vs.* $[C^{++}]$, where C stands for cation

$[C^{++}]$ (mM) Ratio	0	1.0	2.0	3.25	5.0	6.0	7.5	Mean ratios
AR_5/Ar_1	4.08	4.48	4.20	4.50	4.40	4.33	3.89	4.3
AR_4/AR_1	2.84	3.03	2.80	3.08	3.00	3.05	—	2.9
AR_3/AR_1	2.00	2.18	2.33	2.33	2.43	2.56	—	2.3
AR_2/AR_1	1.36	1.58	1.40	1.50	1.66	1.67	—	1.5

Table 2. Conductance levels for a neutral membrane

Substate	$\gamma(\phi_0 = 0)$ pS
AR_1	5[a]
AR_2	7.5
AR_3	11.5
AR_4	14.5
AR_5	21.5

[a] This is the only experiment value; the other numbers are calculated values.

Mg; above 20 mM Mg, the unit conductance of AR_1 remains constant at approximately 5 pS. Large divalent concentrations thus appear to neutralize the surface charge near the channel; 5 pS represents the K conductance through AR_1 in neutral surroundings, in which condition the surface concentration of K equals the bath concentration.

To estimate the lowest conductance of the other substates, which occur only rarely in a neutralized membrane, we divided the conductance of substate AR_x by the conductance of substate AR_1 using Fig. 6. These ratios, listed in Table 1, vary little as the divalent concentration increases. Since the differences between the ratios are unequal, Table 1 provides additional evidence that the higher conductance states are not simply multiples of the lowest state. Assuming the ratios remain constant as divalent concentration increases allows an estimate of the lowest conductance for each substate: the values given in Table 2 appear reasonable, since the curves in Fig. 6 extrapolate to these same conductances for high concentrations of divalent cations. Constant conductance in high divalent concentration is also a feature of reconstituted channels in lipid bilayers (McLaughlin et al., 1971; Apell et al., 1977, 1979*a*,*b*).

The conductance of the neutralized channel furnishes an estimate of the surface potential [Eq. (3)]. The calculation assumes that the conductance of the pore is proportional to the surface concentration of K, which Fig. 3 demonstrates for substrate AR_2. The data in Fig. 3 are obtained by holding ϕ_0 constant as the bath concentration of K varies: if γ is proportional to K_0 then

$$\gamma/\gamma_{100} = K/K_{100}. \quad (5)$$

Table 3 summarizes these calculations: (i) the surface potential becomes less negative as divalent cation concentration increases; (ii) the potential at the surface (133 mM monovalent/zero divalent) is −39.4 mV, a reasonable value based on the macroscopic surface charge literature for K channels [*see* Gilbert and Ehrenstein (1983) for a review].

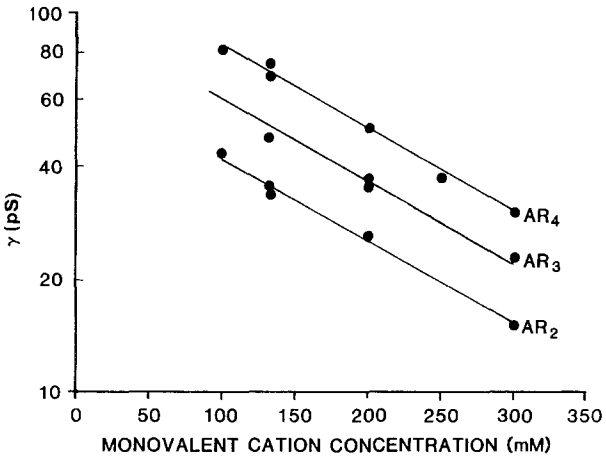

Fig. 7. Effect of monovalent cation concentration on substate conductance. The points represent individual measurements; the lines are empirical fits by eye. All pipette solutions contain 100 mM K and 5 mM EGTA; ionic strength varies by adjusting Na

Monovalent Cations and Channel Conductance

Figure 7 shows the effect of adding impermeable, monovalent cations to divalent-free solutions. Increasing ionic strength with monovalent cations (keeping K = 100 mM) decreases channel conductance. Calculating surface potentials from the monovalent data requires our previous estimates of the neutral membrane conductance. As with the divalents, the monovalent data show that surface potential of all substates is approximately the same for each concentration (Table 4).

Surface Potential and Surface Charge

Figure 8 plots the mean surface potentials *vs.* divalent and monovalent cation concentration. The change in surface potential per tenfold increase in cation concentration is a useful parameter; drawing a tangent to the linear portion of the curves in Fig. 8 gives values of −62 mV for monovalent cations and

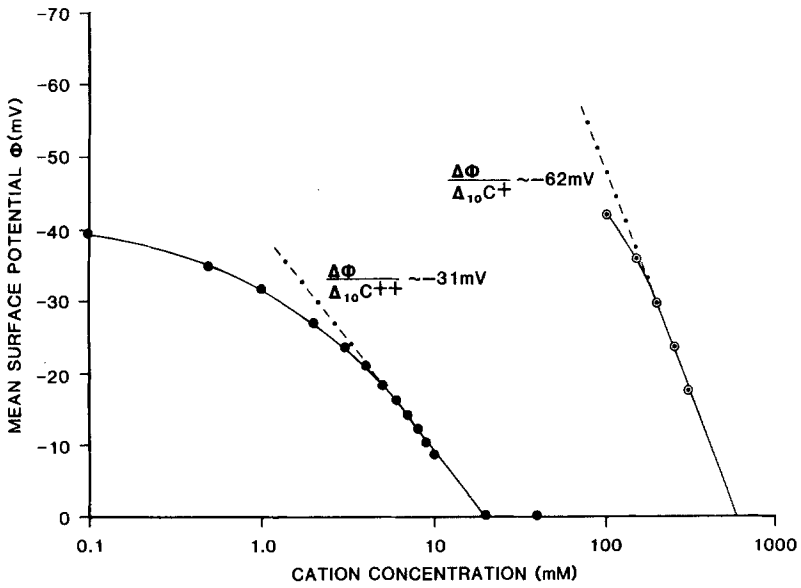

Fig. 8. Mean surface potential ϕ vs. cation concentrations (all substates, Tables 3 and 5). The maximum change in surface potential per 10-fold increase in cation concentration is −31 mV for C^{++} and −62 mV for C^{+}, where C stands for cation

Table 3. Surface potentials for substates of the inward rectifier in the presence of divalent cations[a]

Substate	$[C^{++}]$	γ_K	ϕ_0	Substate	$[C^{++}]$	γ_K	ϕ_0
AR_1	0.0	25.0	−41.0	AR_4	0.0	71.0	−40.4
	0.5	20.0	−35.3		0.5	60.0	−36.1
	1.0	17.0	−31.1		1.0	53.0	−33.0
	2.0	14.0	−26.2		2.0	44.0	−28.2
	3.0	12.0	−22.3		3.0	38.0	−24.5
	4.0	11.0	−20.1		4.0	34.0	−21.7
	5.0	10.0	−17.6		5.0	30.0	−18.5
	6.0	9.4	−16.1		6.0	28.0	−16.7
	7.0	8.6	−13.8		7.0	25.0	−13.9
	8.0	8.0	−12.0		8.0	23.0	−11.7
	9.0	7.3	− 9.6		9.0	21.5	−10.0
	10.0	6.8	− 7.8		10.0	20.0	− 8.2
AR_2	0.0	34.0	−38.5	AR_5	0.0	102.0	−39.6
	0.5	29.0	−34.4		0.5	86.0	−35.3
	1.0	26.0	−31.6		1.0	76.0	−32.1
	2.0	22.0	−27.4		2.0	64.0	−27.8
	3.0	19.5	−24.3		3.0	55.0	−23.9
	4.0	18.0	−22.3		4.0	49.4	−21.0
	5.0	16.5	−20.1		5.0	44.0	−18.2
	6.0	15.0	−17.6		6.0	40.0	−15.8
	7.0	14.0	−15.9		7.0	37.0	−13.8
	8.0	13.0	−14.0		8.0	34.0	−11.7
	9.0	12.0	−12.0		9.0	31.5	− 9.8
	10.0	11.0	− 9.7		10.0	29.0	− 7.6
AR_3	0.0	50.0	−37.4	Mean of all substate	0.0		−39.4
	0.5	44.0	−34.1		0.5		−35.0
	1.0	39.0	−31.1		1.0		−31.8
	2.0	33.0	−26.8		2.0		−27.3
	3.0	29.0	−23.5		3.0		−23.7
	4.0	26.5	−21.2		4.0		−21.3
	5.0	24.0	−18.7		5.0		−18.6
	6.0	22.0	−16.5		6.0		−16.5
	7.0	20.5	−14.7		7.0		−14.4
	8.0	19.0	−12.8		8.0		−12.4
	9.0	17.5	−10.7		9.0		−10.5
	10.0	16.5	− 9.2		10.0		− 8.5

[a] Calculated from data of Fig. 6.

Table 4. Surface potentials for substates of the inward rectifier in the presence of monovalent cations[a]

Substate	C^+	γ_K	ϕ
AR_2	100	41	−43.2
	150	32	−36.9
	200	25	−30.6
	250	19.5	−24.3
	300	15.5	−18.5
AR_3	100	55	−39.8
	150	44	−34.1
	200	35	−28.3
	250	28	−22.6
	300	23	−17.6
AR_4	100	84	−44.7
	150	64	−37.8
	200	50	−31.5
	250	39	−25.2
	300	30	−18.5
Mean	100		−42.6
	150		−36.3
	200		−30.1
	250		−24.0
	300		−18.2

[a] Calculated from data of Fig. 7.

Table 5. Distribution of channels

# Channels in patch	Occurrence	Frequency (%)	Expectation if exponential (%)
1	11	23.9	21.1
2	12	26.1	27.3
3	14	30.4	23.5
4	5	10.9	15.2
5	2	4.3	7.8
6	2	4.3	3.4

Table 6. Frequency of occurrence of at least one particular channel substate in a patch

Substate	Frequency (%)	Expectation if exponential (%)
AR_1	16.2	62
AR_2	35.3	36
AR_3	20.6	22
AR_4	16.2	15
AR_5	11.8	9

−31 mV for divalent cations, near the Gouy-Chapman limits of −58 and −39 mV at 25°C.

From Eq. (4), for our standard solution of 100 K and 33 Na,

$$\sigma_s = -0.25\ e/nm^2. \quad (6)$$

The Gouy-Chapman surface charge surrounding K channels in squid axon, *Myxicola* axon, and toad and frog node ranges between −0.2 and −0.8 e/nm^2 (Mozhagana & Naumov, 1970; Bresmer, 1973; Begenisich & Lynch, 1974; Begenisich, 1975; Vogel, 1974; Wanke, Carbone & Tosta, 1979).

Channel Density and the Occurrence of Substates

Table 5 summarizes the distribution of channels in 46 patches; deleting the first number, the distribution is nearly exponential, suggesting a random placement of the channels in the membrane. The mean number of channels per patch is 2.6. Assuming a patch area of 5.5 μm^2 (*see* Materials and Methods) implies a density of one channel per 2 μm^2, equivalent to the channel density of Sakmann and Trube (1984*a*) for the inward rectifier of adult guinea pig ventricular cells.

Table 6 lists the frequency of encountering at least one substate per patch. The conclusion from these data is that the frequency of seeing substates decreases as their conductance increases. The chance of finding a particular substate decreases exponentially from AR_1 to AR_5 (assuming that the low frequency of observing AR_1 comes about because of its small size and not because of its rarity), suggesting that the free energy for transition is larger to the higher states than to the lower states.

Barium Block

Barium ions in the patch pipette do not absolutely block the inward-rectifier channel in chick embryo heart cells, though Ba may change the kinetics and frequency of appearance of the channels. The inward-rectifier channel opens in concentrations as high as 10 mM external Ba (Fig. 6).

Inward Rectification

The common feature of all AR substates is complete inward rectification; no outward current flows through these channels. Rectification could result from voltage-dependent gates or intrinsic properties of the open pore. Figure 9 shows that mean channel open times are approximately voltage independent and that the channels are open more than 80% of the time. Assuming these data extrapolate to E_K (near $V = 0$), rectification lies not with gate kinetics but within the pore itself. In support of this view, Mat-

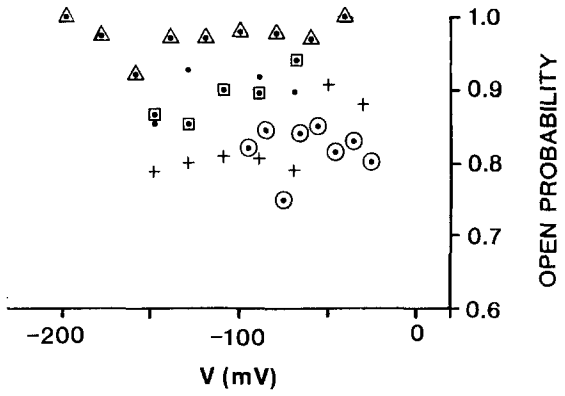

Fig. 9. Effect of membrane voltage on the open-state probabilities. The average open probability is about 90%: the symbols ⊙, +, ⊡, ●, and △ refer to substates AR_1, AR_2, AR_3, AR_4, and AR_5, respectively

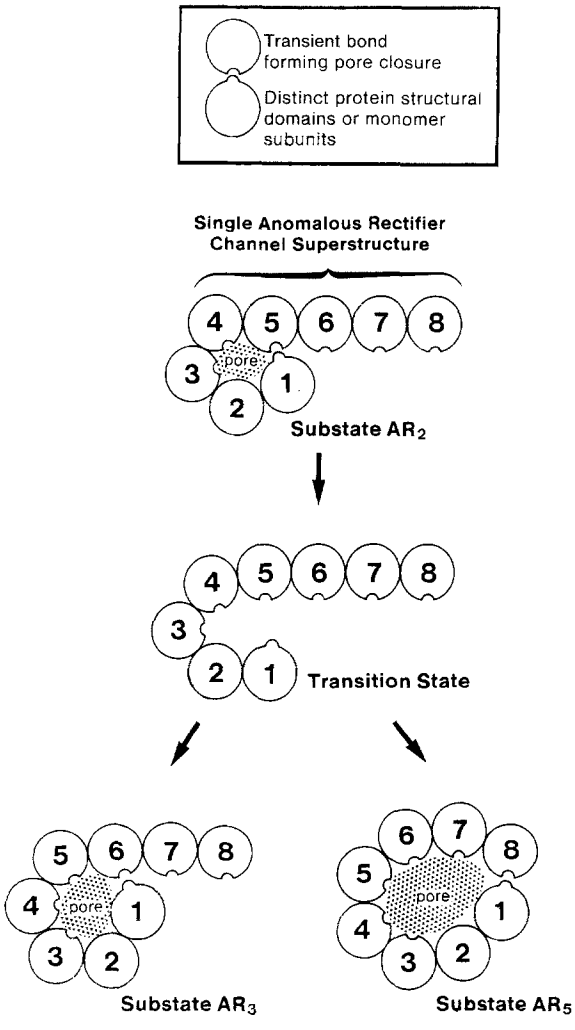

Fig. 10. Model of substate conductances. The closed circles forming the boundaries of the pore represent negatively charged protein monomers or protein domains of the channel. The intrinsic negative charge tends to keep the pore open and enlarged. Adding external cations results in a decrease in surface charge and a partial closing of the open structure

suda, Saigusa and Irisawa (1987) show that in the absence of internal Mg, the inward rectifier does not rectify; in the normal solution, internal Mg probably blocks the open pore and prevents it from conducting an outward current.

Discussion

Since Mg, Ca, and Ba have the same effect on conductance, it is probably the screening of surface charge, and not titration via specific cation binding to the protein, that causes the observed decrease in surface potential. Thus, the embryonic chick heart is similar to *Myxicola* giant axons, which bind neither Ca nor Mg to their external surfaces (Schauf, 1975), but is unlike squid giant axons and frog node preparations, which do show binding for different cations (Frankenhaeuser & Hodgkin, 1957; Hille et al., 1975). In chick AR channels, the divalent cations screen negative surface charge and decrease local surface potential; the more positive the surface potential, the lower the local concentration of permeable cations and the smaller the inward conductance.

For constant ionic strength, the single-channel conductance of at least one of the chick inward-rectifier conduction states is proportional to the first power of the external K concentration. Sakmann and Trube (1984*a*) found a (roughly) square root dependence on K concentration. By substituting K with Na ions, the present experiments attempted to separate the screening effect of K on conductance from the concentration effect of K on conductance. Beating cells have one conduction state with the approximate dependence on K that Sakmann and Trube report (Mazzanti & DeFelice[1]).

The dependence of surface potential on cation concentration in cardiac inward-rectifier K channels is comparable to crayfish axon Na channels (D'Arrigo, 1978), but it is significantly greater than for Na and K channels in virtually all other experiments (Gilbert & Ehrenstein, 1983). Greater sensitivity suggests that electrostatic repulsion helps maintain the open channel and that decreasing the surface charge results in partial collapse of the pore.

The high K selectivity of all substates indicates that conductance and selectivity are independent. The AR channel behaves as a funnel toward the cell interior, with a large opening that can change dimension and a small opening that cannot. Inter-conversions between the closed and the five distinct open states may result from the number of protein

[1] Mazzanti, M., DeFelice, L. K channel kinetics during the spontaneous heartbeat in embryonic chick ventricle cells (*in preparation*).

monomers forming the channel, as in alamethicin. Figure 10 summarizes this view of AR substrates and the transitions from one substate to another.

Although the embryonic chick ventricle AR channel is similar to the mammalian heart AR, these differences exist: (i) Sakmann and Trube (1984*b*) reported a strong dependence of channel open-time on voltage, for example $p = 0.15$ at -50 mV and 0.02 at -110 mV. This decrease of p with negative voltage agrees approximately with Kameyama et al. (1983), but it disagrees with Kurachi (1985) and Trube and Hescheler (1984), who explain inward rectification by a decrease of p with positive voltage. Embryonic chick ventricle AR channels are roughly independent of voltage and have fairly uniform open-time probabilities between about 0.8 and 0.9. (ii) Sakmann and Trube demonstrated a blocking effect of barium, corroborated by Kameyama et al. (1983), and that Ba shortens openings and decreases the number of openings per burst. In Bechem et al. (1983), Ba caused rapid interruptions of open AR channels instead of complete closures. In embryonic chick ventricle, it was possible to study the conductance of AR channels in up to 10 mM Ba. (iii) Finally, Sakmann and Trube relate single-channel conductance to the 0.62 power of K; in embryonic chick ventricle, when the membranes are held at constant ionic strength, the conductance of at least one of the substates is proportional to the 1st power of K concentration.

It is difficult to assign a function to a K channel that conducts no current above E_K. A possible role of inward-rectifier channels in heart may be to counter local elevations in cleft potassium. A topical increase in external K would cause E_K to shift positive with respect to the neighboring membrane potential, allowing the extra K to enter the cell through AR channels. Potassium scavenging might be a way for the cell to reduce transient regional hyperkalemia, and it could lessen cardiac anomalies such as ectopic pacemakers, re-entry arrhythmias, and conduction disorders that occur with metabolic or structural damage to the myocardium. If valid, such a mechanism would depend not only on the concentration of external K, but also on the concentration of Mg and Ca.

We wish to thank Ms. B.J. Duke Cuti for technical assistance in preparing the tissue cultures and Mr. W.N. Goolsby for his expertise in electronics and computer analysis. We are grateful to Dr. Gerald Ehrenstein for critical comments on this work and to Dr. Sally Wolff for editing the manuscript. NIH Grant HL-27385 supports this research.

References

Apell, H.J., Alpes, H., Läuger, P., Bamberg, E. 1979. Effects of electrical charges on the permeability of the gramicidin channel. *In:* Function and Molecular Aspects of Biomembrane Transport. E. Quagliariello, editor. Elsevier, North Holland Biomedical, Amsterdam

Apell, H.J., Bamberg, E., Alpes, H., Läuger, P. 1977. Formation of ion channels by a negatively charged analog of gramicidin A. *J. Membrane Biol.* **31:**171–188

Apell, H.J., Bamberg, E., Läuger, P. 1979. Effects of surface charge on the conductance of the gramicidin channel. *Biochim. Biophys. Acta* **552:**369–378

Bechem, M., Glitsch, H.G., Pott, L. 1983. Properties of an inward rectifying K channel in the membrane of guinea-pig atrial cardio balls. *Pfluegers Arch.* **399:**186–193

Beeler, G.W., Reuter, H. 1977. Reconstruction of the action potential of ventricular myocardial fibers. *J. Physiol. (London)* **268:**177–210

Begenisich, T. 1975. Magnitude and location of surface charges in *Myxicola* giant axons. *J. Gen. Physiol.* **66:**47–65

Begenisich, T., Lynch, C. 1974. Effects of internal divalent cations on voltage-clamped squid axons. *J. Gen. Physiol.* **63:** 675–689

Bell, J., Miller, C. 1984. Effects of phospholipid surface charge on ion conduction in the K channel of sarcoplasmic reticulum. *Biophys. J.* **45:**279–287

Bresmer, T. 1973. Effects of ionic concentration in permeability properties of nodal membrane in myelinated nerve fibers of *Xenopus laevis*. *Acta Physiol. Scand.* **817:**474–484

D'Arrigo, J.S. 1978. Screening of membrane surface charges by divalent cations: An atomic representation. *Am. J. Physiol.* **235:***C*109–*C*117

DeHaan, R.L. 1967. Regulation of spontaneous activity and growth of embryonic chick heart cells in tissue cultures. *Dev. Biol.* **16:**216–249

Fozzard, H.A., Sheu, S.S. 1980. Intracellular potassium and sodium activities of chick ventricular muscle during embryonic development. *J. Physiol. (London)* **137:**218–244

Frankenhaeuser, B., Hodgkin, A.L. 1957. The action of calcium on the electrical properties of squid axons. *J. Physiol. (London)* **137:**245–260

Gilbert, D.L., Ehrenstein, G. 1969. Effect of divalent cations on potassium conductance of squid axons: Determination of surface charge. *Biophys. J.* **9:**447–463

Gilbert, D.L., Ehrenstein, G. 1983. Membrane surface charge. *Curr. Topics Membr. Transp.* **22:**407–421

Grahame, D.C. 1947. The electric double layer and the theory of electrocapillarity. *Chem. Res.* **41:**441–501

Hamill, O., Marty, A., Neher, E., Sakmann, B., Sigworth, F.J. 1981. Improved patch-clamp techniques for high-resolution current recording from cells and cell-free membrane patches. *Pfluegers Arch.* **391:**85–100

Hille, B., Woodhull, A.M., Shapiro, B.I. 1975. Negative surface charge near sodium channels of nerve: Divalent ions, monovalent ions, and pH. *Philos. Trans. R. Soc. London B* **270:** 301–318

Hume, J.R., Uehara, A. 1985. Ionic basis of the different action potential configurations of single guinea-pig atrial and ventricular myocytes. *J. Physiol. (London)* **366:**525–544

Kameyama, M., Kiyosue, T., Soejima, M. 1983. Single current analysis of the inward rectifier K current in the rabbit ventricular cells. *Jpn. J. Physiol.* **33:**1039–1056

Kurachi, Y. 1985. Voltage dependent activation of the inward rectifier potassium channel in the ventricular cell membrane of guinea-pig heart. *J. Physiol. (London)* **366:**365–385

Matsuda, H., Saigusa, A., Irisawa, H. 1987. Ohmic conductance through the inwardly rectifying K channel and blocking by internal Mg. *Nature (London)* **325:**156–159

McDonald, T.F., DeHaan, R.L. 1973. Ion levels and membrane potential in chick heart tissue and cultured cells. J. Gen. Physiol. **61:**89–109

McDonald, T.F., Trautwein, W. 1978*a*. Membrane currents in cat myocardium: Separation of inward and outward components. *J. Physiol. (London)* **247:**193–216

McDonald, T.F., Trautwein, W. 1978*b*. The potassium current underlying delayed rectification in cat ventricular muscle. *J. Physiol. (London)* **274:**217–246

McLaughlin, S.G., Szabo, G., Eisenman, G. 1971. Divalent ions and the surface potential of charged phospholipid membranes. *J. Gen. Physiol.* **58:**667–687

Mozhagana, G.N., Naumov, A.P. 1970. Effect of surface charge on the steady stage potassium conductance of nodal membrane. *Nature (London)* **228:**164–165

Sakmann, B., Neher, E. 1983. General parameters of pipettes and membrane patches. *In:* Single-Channel Recording. B. Sakmann and E. Neher, editors. Plenum, New York

Sakmann, B., Trube, G. 1984*a*. Conductance properties of single inwardly rectifying potassium channels in ventricular cells from guinea-pig heart. *J. Physiol. (London)* **347:**641–657

Sakmann, B., Trube, G. 1984*b*. Voltage-dependent inactivation of inwardly-rectifying single-channel currents in the guinea-pig heart cell membrane. *J. Physiol. (London)* **347:**659–683

Schauf, C.L. 1975. The interactions of calcium with *Myxicola* giant axons and a description in terms of a simple surface charge model. *J. Physiol. (London)* **248:**613–624

Schmid, R.W., Reilley, C.N. 1957. New complexon for titration of calcium in the presence of magnesium. *Anal. Chem.* **29:** 264–268

Trube, G., Hescheler, J. 1984. Inward rectifying channels in isolated patches of the heart cell membrane: ATP-dependence and comparison with cell-attached patches. *Pfluegers Arch.* **401:**178–184

Vogel, W. 1974. Calcium and lanthanum effects at nodal membrane. *Pfluegers Arch.* **350:**25–39

Wanke, E., Carbone, E., Tosta, P.L. 1979. K conductances modified by a titratable group accessible to protons from the intracellular side of the squid giant axon. *Biophys. J.* **26:**319–324

Received 12 August 1987; revised 15 December 1987